Microarray Identifies Extensive Downregulation of Noncollagen Extracellular Matrix and Profibrotic Growth Factor Genes in Chronic Isolated Mitral Regurgitation in the Dog

Junying Zheng, PhD; Yuanwen Chen, MD, PhD; Betty Pat, PhD; Louis A. Dell'Italia; Michael Tillson, DVM; A. Ray Dillon, DVM; Pamela C. Powell, MS; Ke Shi, MD; Neil Shah, MS; Thomas Denney, PhD; Ahsan Husain, PhD; Louis J. Dell'Italia, MD

Background—The volume overload of isolated mitral regurgitation (MR) in the dog results in left ventricular (LV) dilatation and interstitial collagen loss. To better understand the mechanism of collagen loss, we performed a gene array and overlaid regulated genes into ingenuity pathway analysis.

Methods and Results—Gene arrays from LV tissue were compared in 4 dogs before and 4 months after MR. Cine-magnetic resonance–derived LV end-diastolic volume increased 2-fold ($P=0.005$), and LV ejection fraction increased from 41% to 53% ($P<0.007$). LV interstitial collagen decreased 40% ($P<0.05$) compared with controls, and replacement collagen was in short strands and in disarray. Ingenuity pathway analysis identified Marfan syndrome, aneurysm formation, LV dilatation, and myocardial infarction, all of which have extracellular matrix protein defects and/or degradation. Matrix metalloproteinase-1 and -9 mRNA increased 5- ($P=0.01$) and 10-fold ($P=0.003$), whereas collagen I did not change and collagen III mRNA increased 1.5-fold ($P=0.02$). However, noncollagen genes important in extracellular matrix structure were significantly downregulated, including decorin, fibulin 1, and fibrillin 1. In addition, connective tissue growth factor and plasminogen activator inhibitor were downregulated, along with multiple genes in the transforming growth factor-β signaling pathway, resulting in decreased LV transforming growth factor-β1 activity ($P=0.03$).

Conclusions—LV collagen loss in isolated, compensated MR is chiefly due to posttranslational processing and degradation. The downregulation of multiple noncollagen genes important in global extracellular matrix structure, coupled with decreased expression of multiple profibrotic factors, explains the failure to replace interstitial collagen in the MR heart. **(*Circulation*. 2009;119:2086-2095.)**

Key Words: extracellular matrix ■ gene expression microarray analysis ■ left ventricle ■ mitral regurgitation ■ TGF-beta

The extracellular matrix (ECM) is a heterogeneous amalgam of macromolecules that are capable of self-assembly into a multimeric structure that contributes to the scaffolding of cells in the heart. In addition to collagen, the multimeric structure contains molecules that stabilize collagen and contribute to integrity of the entire ECM by connecting individual cardiomyocytes and cardiomyocyte bundles in a laminar structure. This structural organization maintains ventricular shape and provides for transmission of forces during systole across the myocardial wall.[1] An intact ECM is maintained in pressure overload. However, over time, pressure overload produces concentric left ventricular (LV) and cardiomyocyte hypertrophy and LV fibrosis.[2] In contrast, the volume overload of isolated mitral regurgitation (MR) in the dog produces eccentric LV remodeling, which is characterized by LV dilation and wall thinning, cardiomyocyte elongation, and a decrease in interstitial collagen.[3–5] We have shown that interstitial collagen loss within 12 hours after the volume overload of aortocaval fistula in the rat causes LV dilatation. This precedes cardiomyocyte elongation, suggesting that collagen breakdown is the first step in the pathophysiology of LV dilatation in response to a pure volume overload.[6]

Clinical Perspective p 2095

Evidence from our dog model of isolated MR suggests that persistent loss of interstitial collagen is central to chronic

Received October 5, 2008; accepted January 30, 2009.

From the Center for Heart Failure Research, Departments of Medicine (J.Z., Y.C., B.P., L.A.D., P.C.P., K.S., N.S., A.H., L.J.D.) and Physiology and Biophysics (A.H.), University of Alabama at Birmingham; Birmingham Department of Veteran Affairs, Birmingham, Ala (L.J.D.); and Auburn University College of Veterinary Medicine (M.T., A.R.D.) and School of Engineering (T.D.), Auburn, Ala.

The online-only Data Supplement is available with this article at http://circ.ahajournals.org/cgi/content/full/CIRCULATIONAHA.108.826230/DC1.

Reprint requests to Louis J. Dell'Italia, MD, University of Alabama at Birmingham Center for Heart Failure Research, Division of Cardiology, 434 BMR2, 1530 3rd Ave S, Birmingham, AL 35294-2180. E-mail loudell@uab.edu

Circulation **is available at http://circ.ahajournals.org** **DOI: 10.1161/CIRCULATIONAHA.108.826230**

Table 1. Primer Sequences for Validating Microarray by Real-Time PCR

Gene Name	Forward Primer	Reverse Primer	Genebank ID
MMP1	5′gtgcctcctacaagatagca3′	5′cgttgattttctttaccctctgc3′	XM_849520.1
MMP9	5′ggcaaattccagacctttgag3′	5′tacacgcgagtgaaggtgag3′	NM_001003219.1
GAPDH	5′gaacatcatccctgcttccac3′	5′accacctggtcctcagtgta3′	NM_001003142.1
PAI-1	5′tcaagaggtgctgtatgtgt 3′	5′ccatgaaaaggactgttcct 3′	XM_844252.1
TGF-βR2	5′caaggccaagctgaagcagaa3′	5′tgacatgccgagtgaggtact3′	XM_534237
TGF-βR3	5′ctacctgcaaggccaagatga3′	5′tcaggtcggctgaagaaggaa3′	XM_547284.2
Lumican	5′cagatggccaaactgccttct3′	5′gttctcattgacagtcggtatg3′	XM_539716
Decorin	5′tgaaccagatgatcgtcgtaga3′	5′ggctagatgcatcaaccttggt3′	NM_001003228.1
Fibrillin	5′cttttgcaagtgtcctcctggtt3′	5′tgctctgatgggacacatctca3′	XM_535468.2
KITLG	5′agattccagagtcagtgtcacaa3′	5′ctgtccttgtgagatttggttgt3′	NM_001012735.1
VWF1	5′gtcacttctgcaaggtcaatga3′	5′atgtccacttcctcttcagact3′	NM_001002932.1
Fibulin1	5′cacagaggacaatgactgcaa3′	5′ cacgttcttctggcatgtgta3′	XM_531698.2

eccentric LV and cardiomyocyte remodeling, but the molecular basis remains unclear. This is an important question because currently no recommended medical therapy is available to attenuate LV remodeling and thereby delay the need for valve surgery in patients with isolated MR.[7] Chronic angiotensin-converting enzyme inhibition[5,8] and angiotensin II receptor blockade,[9] which reduce cardiomyocyte remodeling and collagen accumulation in pressure overload, do not attenuate LV dilatation, cardiomyocyte elongation, and interstitial collagen loss in the dog model of isolated MR. This illustrates that concentric remodeling in pressure overload and eccentric remodeling in isolated MR have different underlying mechanisms of ECM turnover and synthesis.

We have shown that eccentric LV remodeling in isolated, compensated MR is associated with increased matrix metalloproteinase (MMP) activity, loss of interstitial collagen, and cardiomyocyte elongation.[4,5] Animal models of aortocaval fistula in the rat and pacing tachycardia in the pig have shown that MMP inhibition significantly attenuates LV dilatation by preventing interstitial collagen loss, implicating collagen degradation in the pathophysiology of LV remodeling and heart failure.[10,11] Here, we report a more global defect of ECM homeostasis. Using gene array, we not only found marked increases in MMP gene expression but also significant decreases in the expression of critical noncollagen ECM scaffolding protein and glycoprotein genes, as well as a decreased expression of multiple profibrotic growth factors in the LV myocardium of dogs with chronic isolated MR.

Methods

Creation of MR

Mitral valve regurgitation was induced at Auburn University College of Veterinary Medicine in conditioned mongrel dogs of either sex (weight, 19 to 26 kg) by chordal rupture as described previously in our laboratory.[3–5,9] Magnetic resonance imaging (MRI) and LV hemodynamics were performed in all dogs before MR induction and after 4 months of MR under isoflurane anesthesia. Biopsies were taken from the LVs of each dog before induction of MR. Animals were transported to the University of Alabama at Birmingham for the terminal experiments. This study was approved by the Animal Resource Programs at University of Alabama at Birmingham and Auburn University College of Veterinary Medicine.

Magnetic Resonance Imaging

Dogs were anesthetized with isoflurane anesthesia, and cine-MRI was performed with a Picker Vista 1.0-T magnet. Endocardial and epicardial contours were traced manually on the LV end-diastolic (ED) and end-systolic (ES) images. The contours were traced to exclude the papillary muscles. LVED and LVES volumes were determined by summing serial short-axis slices as described previously in our laboratory.[3,5]

Euthanasia Study

Dogs were maintained under a deep plane of isoflurane anesthesia and were mechanically ventilated (Harvard Apparatus, Inc). The heart was arrested as described previously in our laboratory.[3,5] The LV was cut into pieces that were either perfusion-fixed with 3% paraformaldehyde, snap-frozen in liquid nitrogen, or placed in an RNA stabilizing solution (RNA later, Qiagen Sciences) for subsequent analyses.

RNA Isolation

Total RNA was extracted from LV biopsies before MR induction and at 4 months of MR with the Qiagen RNeasy Fibrous Tissue Mini Kit (Qiagen Sciences). DNase I (Qiagen Sciences) was applied to remove genomic contamination. Negative reverse transcription polymerase chain reaction (RT-PCR) with the use of GAPDH primers (Table 1) ensured no genomic contamination. Integrity of the RNA was evaluated on the BioRad Experion (Bio-Rad Laboratories, Hercules, Calif). Samples with optical density ratio 260/280 $>$1.8, 28S/18S $>$1.5 were selected for microarray processing.

Microarray Analysis

Two-color microarrays were performed on Agilent 4$\times$44 canine array chips with 42 000+ predicted *Canis familiari* genes following established Agilent 2-color protocol (Agilent Technologies). Comparative analysis between expression profiles for Agilent experiments was performed with the use of Genespring GX 7.3.1 (Agilent Technologies). Gene expression data were normalized in 2 ways: per chip normalization and per gene normalization. Dye swap hybridizations were merged with their counterparts, with the average of the 2 values for a spot taken as the representative value. A gene list was generated containing a 24 196 gene sequences flagged as present. The "present" list was then filtered with the use of "filter by expression," "self confidence," and "Benjamini and Hochberg false discovery test." Significant genes were selected with a cutoff of $P<0.05$ and fold change $>$1.5.

Ingenuity Pathway Analysis

The selected genes were subsequently analyzed with the use of ingenuity pathway analysis (IPA) 5.0 (Ingenuity Systems Inc).

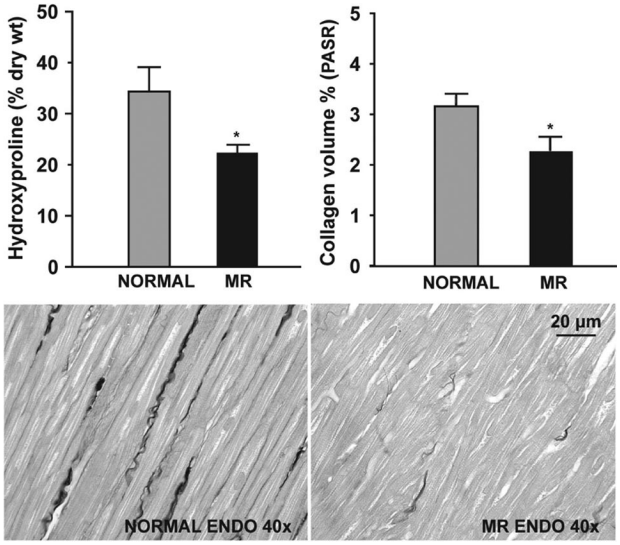

Figure 1. Total collagen (% dry weight tissue) in the LV of MR vs normal dogs (left) and volume percentage collagen by picric acid sirius red (right) with marked loss of interstitial collagen in MR dog (bottom). MR: n=5; normal: n=4.

Functions and pathways, which were predicted to be influenced by the differentially expressed genes, were ranked in order of significance and further analyzed by overlaying with cardiovascular function and disease.

Verification of Gene Expression With Real-Time RT-PCR

Quantitative real-time PCR was performed with the use of the Bio-Rad iCycler iQ system (Bio-Rad Laboratories) on 500 ng total RNA from microarray samples to verify array data. Selected genes and primer sequences (Sigma-Genosys, Woodlands, Tex) are presented in Table 1. GAPDH was chosen as an endogenous control.

Western Blot for Decorin, Integrin α_V, Transforming Growth Factor-β Receptor 2, Smad7, and Phospho-Smad2

Forty micrograms of total protein from LV endocardium of normal and 4-month MR dogs was subjected to sodium dodecyl sulfate–polyacrylamide gel electrophoresis followed by Western blot analysis. Primary antibodies used were decorin (H-80) (Santa Cruz Biotechnology, Inc, Santa Cruz, Calif), integrin α_V (Abcam, Cambridge, Mass), transforming growth factor (TGF)-β receptor 2 (TGF-βR2) (C-16) (Santa Cruz Biotechnology, Inc), smad7 (Santa Cruz Biotechnology), and phospho-smad2 (Ser465/467) (Upstate Cell Signaling Solutions, NY), respectively. Membranes were stripped and reblotted with anti-tubulin (Sigma-Aldrich, St Louis, Mo) as a loading control.

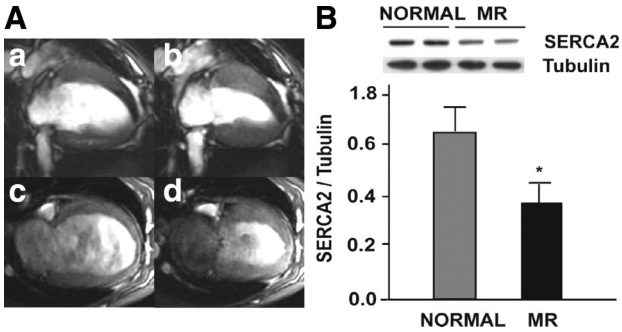

Figure 2. A, Representative MRI demonstrating normal dog (a and b) compared with MR (c and d) with increased LVED volume and wall thinning with the LV changing from a conical to spherical shape in MR. Note the diffuse black signal void of MR and enlarged left atrium. B, Western blot demonstrates decreased SERCA2 in MR (n=5) vs normal (n=4).

Table 2. MRI LV Volumes and Function in Dogs Before (Baseline) and 4 Months After Induction of MR

	Baseline	MR	*P*
LVED volume, mL	34±4	64±9	0.005
LVES volume, mL	20±4	31±8	0.027
LVED diameter, mm	34±2	42±3	0.004
LVES diameter, mm	28±2	32±2	0.007
Stroke volume, mL	13±1	33±2	0.006
Ejection fraction, %	41±5	53±6	0.007
Sample size, n	4	4	

Immunohistochemistry for Phospho-Smad2 and Mast Cells Chymase

Immunohistochemistry was performed on formalin-fixed, paraffin-embedded LV endocardium with the use of antibodies for phospho-smad2 (Ser465/467) (Upstate Cell Signaling Solutions) and dog chymase (kindly provided by Dr George H. Caughey, University of California, San Francisco) in normal and 4-month MR dogs. Mast cells were stained with dog chymase antibody and counted for 36 fields randomly chosen at ×40. Total mast cell number was divided by the tissue area to yield the number of mast cells per square millimeter.

TGF-β_1 Activity

Sixty to 100 mg LV endocardium and epicardium were homogenized in PBS (pH 7.4) containing complete protease inhibitor (Roche Diagnostics, Mannheim, Germany) and centrifuged at 12 000*g* for 10 minutes. Total protein in the supernatant was measured with a Bradford protein assay kit (Bio-Rad Laboratories). TGF-β_1 activity was determined by a commercial enzyme-linked immunosorbent assay kit (R&D Systems, Minneapolis, Minn). TGF-β_1 activity was expressed per milligram of protein in each sample.

Total Collagen Analysis

LV endocardial total collagen was determined by the hydroxyproline method according to a previously described colormetric method.[12] Morphological evaluation of volume percent collagen was performed on tissues from normal dogs and 4-month MR dogs by picric acid sirius red as described previously in our laboratory.[13]

Statistical Analysis

Data are presented as mean±SEM. Comparison within groups (magnetic resonance LV volumes) was tested by paired *t* test (RT-PCR) or unpaired *t* test between control and MR dogs (Western

Table 3. Hemodynamic Data Obtained in Dogs Before (Baseline) and 4 Months After Induction of MR

	Baseline	MR	*P*
Cardiac output, L/min	4.14±0.56	3.14±0.44	0.005
LVED pressure, mm Hg	10±2	19±3	0.03
LVES pressure, mm Hg	110±5	107±4	0.67
LV +dP/dT, mm Hg/s	2676±198	2553±377	0.58
LV −dP/dT, mm Hg/s	2637±127	2511±147	0.2
Sample size, n	4	4	

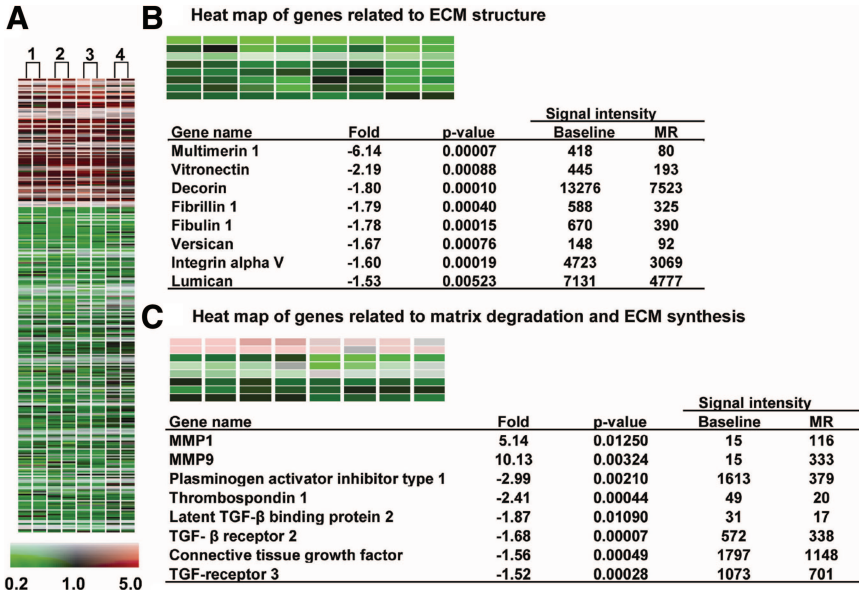

Gene name	Fold	p-value	Signal intensity Baseline	MR
Multimerin 1	-6.14	0.00007	418	80
Vitronectin	-2.19	0.00088	445	193
Decorin	-1.80	0.00010	13276	7523
Fibrillin 1	-1.79	0.00040	588	325
Fibulin 1	-1.78	0.00015	670	390
Versican	-1.67	0.00076	148	92
Integrin alpha V	-1.60	0.00019	4723	3069
Lumican	-1.53	0.00523	7131	4777

Gene name	Fold	p-value	Signal intensity Baseline	MR
MMP1	5.14	0.01250	15	116
MMP9	10.13	0.00324	15	333
Plasminogen activator inhibitor type 1	-2.99	0.00210	1613	379
Thrombospondin 1	-2.41	0.00044	49	20
Latent TGF-β binding protein 2	-1.87	0.01090	31	17
TGF- β receptor 2	-1.68	0.00007	572	338
Connective tissue growth factor	-1.56	0.00049	1797	1148
TGF-receptor 3	-1.52	0.00028	1073	701

Figure 3. A, Heat map of the 659 genes altered >1.5-fold ($P<0.05$) in the 4 MR dogs vs baseline.[1–4] Two-color gene array with dye swap was applied. Red indicates upregulation; black, no change; green, downregulation vs baseline with scale of color corresponding to fold change. B, Genes altered in MR related to ECM structure. C, Genes altered related to TGF-β pathway and ECM degradation.

blot, collagen analysis). A P value of <0.05 was considered statistically significant.

The authors had full access to and take full responsibility for the integrity of the data. All authors have read and agree to the manuscript as written.

Results

Morphometry, MRI, and Hemodynamics

LV mass to body weight ratio increased in MR versus normal dogs (3.9±0.2 to 4.9±0.3 g/kg; $P=0.04$). Total LV endocardial collagen by hydroxyproline was decreased 35% ($P<0.05$), and interstitial collagen volume fraction decreased 40% ($P<0.05$) in 4-month MR dogs versus normal dogs (Figure 1). Hemodynamics and LV volumes and function were recorded before MR induction and 4 months after MR at the time of euthanasia. In MR dogs, LVED volume increased from 34±4 to 64±9 mL ($P<0.005$) as LVES volume increased from 20±4 to 31±8 mL ($P<0.03$), resulting in a 3-fold increase in stroke volume (13±1 to 33±2 mL; $P<0.006$). Cardiac output decreased from 4.14±0.56 to 3.14±0.44 L/min ($P<0.005$) as LVES pressure remained unchanged from baseline, suggesting a decrease in LV function, consistent with a decrease in SERCA2 expression (Figure 2). LVED pressure increased from 10±2 to 19±3 mm Hg ($P<0.03$), and LV $\pm dP/dt_{max}$ did not change; however, LV ejection fraction increased from 41±5% to 53±6% ($P<0.007$) after 4 months of MR (Tables 2 and 3).

Microarray Analysis

A total of 659 genes were differentially expressed by at least 1.5-fold in MR dogs ($P<0.05$), including 217 upregulated and 442 downregulated genes. The heat map in Figure 3A demonstrates a consistent pattern of change of these genes in the 4 MR dogs. Table 4 lists genes well established in the pathophysiology of cardiovascular disease that were altered >1.5-fold. Figure 3B lists noncollagen ECM genes that were downregulated >1.5-fold. These include microfibrillar genes fibrillin 1 and fibulin 1 and glycoprotein genes including multimerin 1, vitronectin, decorin, versican, and lumican. In addition, significant downregulation of integrin α_V occurs. Plasminogen activator inhibitor type 1 (PAI-1), thrombospondin 1, TGF-βR2, TGF-β receptor 3 (TGF-βR3), and connective tissue growth factor (CTGF) are significantly downregulated, whereas MMP-1 and MMP-9 are increased 5- and 10-fold, respectively (Figure 3B, 3C).

Validation of Microarray With Quantitative PCR

Table 5 demonstrates the validation of the microarray results for von Willebrand factor, TGF-βR2, TGF-βR3, fibulin 1, lumican, fibrillin 1, decorin, PAI-1, KITLG, MMP-1, and MMP-9 by quantitative RT-PCR.

Clustering Gene Expression Patterns

The 659 canine genes that changed >1.5-fold were matched to the human ID according to their sequence identity, and 322 genes were mapped in IPA, resulting in a network score of 52 for dermatological diseases (Figure 4). Genes in this network collectively define an association between ECM loss and edema in skin diseases, such as bullous pemphigoid, that are mast cell dependent. Indeed, we found an increase in mast cell numbers in these MR dogs (Figure 5), as reported previously in our laboratory.[4,5] Overlaying this network with cardiovascular function and disease identified Marfan syndrome, aneurysm formation, LV dilatation, vascular injury, and myocardial infarction, all of which are characterized by ECM protein defects, degradation, or both.

Quantification of Integrin α_V, Decorin Protein, and TGF-β_1 Activity

Integrin α_V protein expression was significantly decreased in 4-month MR versus normal dogs (Figure 6A), and decorin protein demonstrated a strong trend to decrease in MR dogs ($P=0.08$) (Figure 6B). Phospho-smad2 was significantly decreased in the MR LV (Figure 7A through 7C) and is in a nuclear location, as demonstrated in Figure 7B. Protein expression of TGF-βR2 (Figure 7D) was significantly decreased in MR versus normal dogs. Smad7 (Figure 7E), which is a negative regulator of TGF-β_1 activity, was

Table 4. Selected Cardiovascular Genes Altered >1.5-Fold in 4-Month MR vs Baseline

Name	Fold	*P*	Description
PPBP	13.03	0.000528	Proplatelet basic protein (chemokine (C-X-C motif) (ligand 7)
MMP-9	10.13	0.003240	*Canis familiaris* matrix metalloproteinase 9
SELL	6.10	0.001850	L-selectin
MMP-1	5.14	0.012500	Matrix metalloproteinase 1 precursor
SELP	3.96	0.000566	Cell adhesion molecule (GMP140)
ANF	3.74	0.015700	Atrial natriuretic factor precursor
BNP	3.68	0.003860	Natriuretic peptides B precursor
ATF3	2.58	0.017200	cAMP-dependent transcription factor ATF-3
CNP	2.49	0.000053	Natriuretic peptide precursor C
BDNF	2.19	0.011500	Brain-derived neurotrophic factor
PDE4D	2.00	0.003880	cAMP-specific phosphodiesterase 4D
KITLG	1.93	0.000336	Stem cell factor
CXCR4	1.75	0.000057	Chemokine (C-X-C motif) receptor 4
EPHB3	1.70	0.002760	EPH receptor B3
PLA2G4A	1.68	0.024900	Cytosolic phospholipase A2
LECT1	1.66	0.001030	Leukocyte cell–derived chemotaxin 1
COL3A1	1.51	0.015900	Collagen, type III, α1
GPIX	1.53	0.015900	Canine platelet glycoprotein IX precursor
IL15	1.50	0.001220	Interleukin 15
TGFBR3	−1.52	0.000275	Transforming growth factor-β receptor 3
LUM	−1.53	0.005230	Lumican
MICAL-L1	−1.54	0.022800	MICAL-like 1
CTGF	−1.56	0.000486	Connective tissue growth factor
PDE9A	−1.56	0.000208	Phosphodiesterase 9A
ADORA2B	−1.58	0.000450	Adenosine A2b receptor
ITGAV	−1.60	0.000190	Integrin α_V
EGFR	−1.61	0.000070	Epidermal growth factor receptor
PDE5	−1.64	0.036500	3′,5′-cGMP phosphodiesterase
ADM	−1.64	0.000057	Adrenomedullin
LAMC2	−1.64	0.002270	Laminin-5 γ2
F3	−1.64	0.024200	Tissue factor (TF)
PPL	−1.66	0.024200	Periplakin
CSPG2	−1.67	0.000755	Chondroitin sulfate proteoglycan 2 (versican)
FLT1	−1.67	0.000093	Fms-related tyrosine kinase 1
VWF	−1.68	0.000077	von Willebrand factor
TGFBR2	−1.68	0.000070	Transforming growth factor-β receptor 2
IDH1	−1.69	0.000033	Cytosolic $NADP^+$–dependent isocitrate dehydrogenase
CA4	−1.71	0.001140	Carbonic anhydrase IV precursor
TLR4	−1.77	0.000457	Toll-like receptor 4 protein
PDGFRA	−1.78	0.000069	Platelet-derived growth factor receptor-α
FBLN1	−1.78	0.000147	Fibulin 1
FBN1	−1.79	0.000404	Fibrillin 1
EFEMP1	−1.79	0.005620	EGF-containing fibulin-like extracellular matrix protein 1
DCN	−1.80	0.000096	Decorin
STC1	−1.83	0.011300	Stanniocalcin 1
LTBP2	−1.87	0.010900	Latent TGF-β binding protein 2
PDPN	−1.88	0.000290	Podoplanin
C1QA	−1.89	0.000302	Complement component 1, q subcomponent, A chain

(*Continued*)

Table 4. Continued

Name	Fold	*P*	Description
GNAQ	−1.91	0.032700	Guanine nucleotide binding protein, q polypeptide
BPI	−1.92	0.000056	Bactericidal/permeability-increasing protein
CTSS	−2.00	0.000004	Cathepsin S
ITGA11	−2.01	0.004970	Integrin α_{11}
PPET3	−2.05	0.002020	Preproendothelin-3
MATN2.	−2.11	0.033600	Matrilin 2 precursor
VTN	−2.19	0.000882	Vitronectin
ITGAX	−2.16	0.007810	Integrin α_X
GRIA4	−2.31	0.001580	Glutamate receptor inotropic, AMPA 4
MSR1	−2.38	0.000034	Macrophage scavenger receptor 1
FGFR2	−2.38	0.019000	Fibroblast growth factor receptor 2
THBS1	−2.41	0.000439	Thrombospondin 1
ICAM1	−2.65	0.021300	Intercellular adhesion molecule 1 (CD54)
PAI-1	−2.99	0.002100	Plasminogen activator inhibitor type 1
CSF1R	−3.76	0.000154	Colony stimulating factor 1 receptor
MMRN1	−6.14	0.000070	Multimerin 1

upregulated and TGF-β_1 activity (Figure 7F) was decreased in MR LV.

Discussion

LV dilatation and remodeling have been associated with a breakdown of interstitial collagen and increased expression and activation of MMPs in models of heart failure[10,11] and in isolated MR.[3–5] Here, for the first time, we report a global decrease in the ECM with downregulation of multiple noncollagen microfibrillar and glycoprotein genes essential to collagen assembly and total ECM structure. Furthermore, in the face of increased expression of MMP genes, expression decreases of growth factor genes and the TGF-β signaling pathway that control synthesis of these ECM components. This could explain the failure of orderly replacement of interstitial collagen, resulting in cardiomyocyte and myofiber slippage and adverse eccentric LV remodeling in isolated MR.

Table 5. Comparison of Selected Genes Identified as Upregulated or Downregulated After 4 Months of MR by Microarray and Quantitative RT-PCR

Gene Name	Fold Change (Microarray)	*P* (Microarray)	Fold Change (QRT-PCR)	*P* (QRT-PCR)
VWF	−1.68	0.00008	−1.52	0.0270
TGFßR2	−1.68	0.00007	−1.50	0.0030
TGFßR3	−1.52	0.00028	−2.30	0.0049
Fibulin1	−1.78	0.00015	−1.73	0.0040
Lumican	−1.53	0.00523	−1.53	0.0130
Fibrillin	−1.79	0.00040	−1.78	0.0280
Decorin	−1.80	0.00010	−1.80	0.0012
PAI-1	−2.99	0.00210	−3.00	0.0100
KITLG	1.93	0.00034	2.63	0.0018
MMP-1	5.14	0.01250	7.00	0.0300
MMP-9	10.13	0.00324	11.00	0.0001

QRT-PCR indicates quantitative RT-PCR.

The 4-month stage of MR has a 2-fold increase in LVED volume but an increase in LV ejection fraction, supporting a relatively compensated state rather than overt failure. IPA identified Marfan syndrome, aneurysm formation, myocardial infarction, and LV dilatation (Figure 4). All of these disorders are marked by ECM protein defects and/or ECM degradation. Indeed, MMP-1 and -9 are highly upregulated and occupy a central location in the IPA map in Figure 4; however, a striking downregulation of multiple essential noncollagen ECM genes also occurs (Figure 3B). Of these genes, decorin is the most abundant in the normal heart and is associated with all major types of collagens.[14] It colocalizes with large helical collagen fibers[15] and binds to specific sites on collagen molecules as they assemble, increasing the tensile strength of uncross-linked collagen fibers.[16] Decorin-null mice have more severe LV dilation after experimentally induced myocardial infarction.[17] In our MR dogs, collagen I mRNA was unchanged and collagen IIIα1 mRNA was increased 1.5-fold, whereas total collagen was decreased by 35%, suggesting a posttranslational degradation. Analysis of collagen showed diffuse endomysial collagen loss with short strands randomly distributed in the LV (Figure 1). With the decrease in decorin mRNA and protein in the MR LV, it is tempting to speculate that decreased decorin resulted in less stable collagen, making it more prone to degradation, which is identified as a direct interaction of MMP-9 on decorin by IPA (Figure 4).

The ECM is made of a collection of noncollagen microfibrils and glycoproteins that serve to connect collagen to cell surfaces and promote cell-cell interactions. Fibrillin 1 is the major component of extracellular microfibrils distributed throughout perivascular and perimysial areas.[18] Fibrillin-1 gene mutations are responsible for Marfan syndrome,[19] whereas fibulins are implicated in elastic matrix fiber assem-

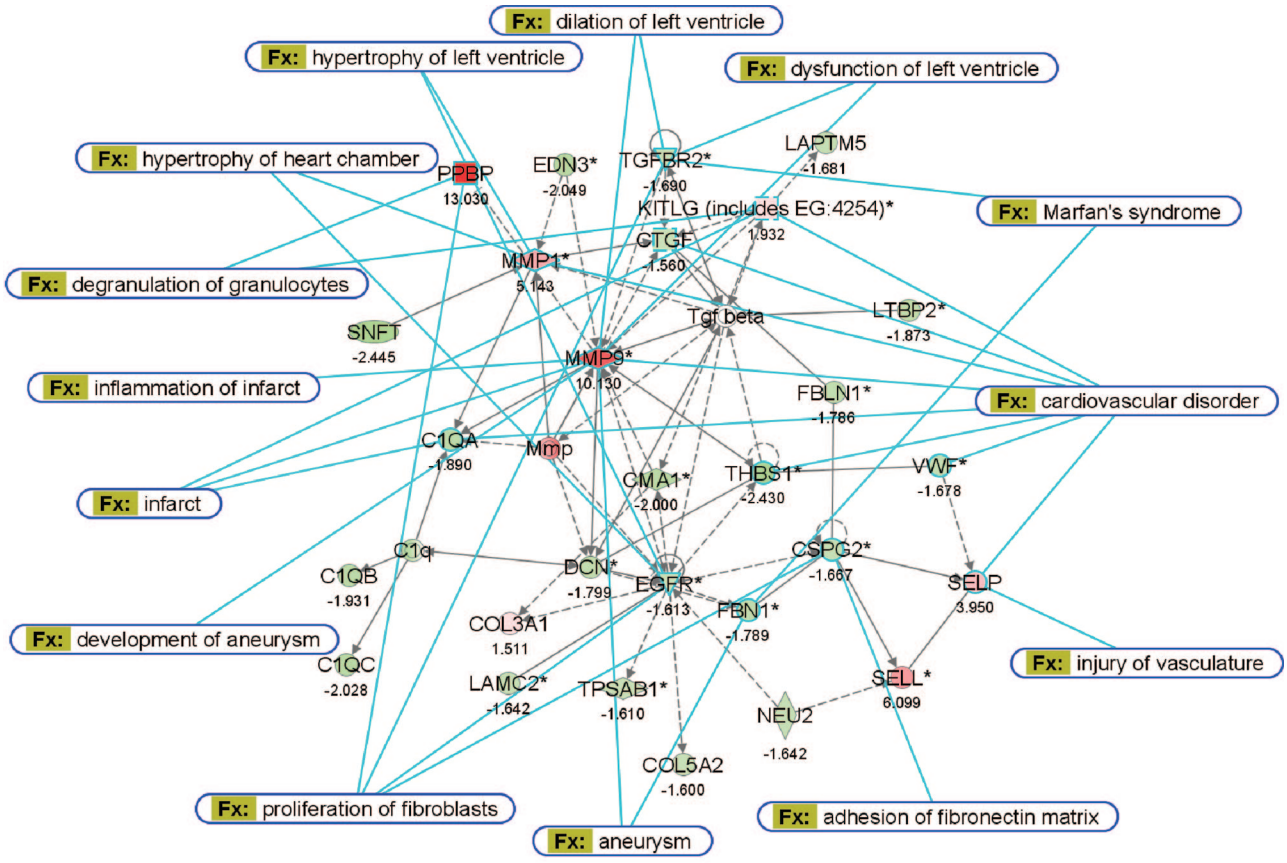

Name	Description	Name	Description
C1QA	complement component 1, q subcomponent, A chain	LAMC2	laminin, gamma 2
C1QB	complement component 1, q subcomponent, B chain	LAPTM5	lysosomal associated multispanning membrane protein 5
C1QC	complement component 1, q subcomponent, C chain	LTBP2	latent transforming growth factor beta binding protein 2
CMA1	chymase 1, mast cell	MMP1	matrix metallopeptidase 1
COL3A1	collagen, type III, alpha 1	MMP9	matrix metallopeptidase 9
COL5A2	collagen, type V, alpha 2	NEU2	sialidase 2 (cytosolic sialidase)
CSPG2	versican	PPBP	pro-platelet basic protein (chemokine (C-X-C motif) ligand 7)
CTGF	connective tissue growth factor	SELL	selectin L (lymphocyte adhesion molecule 1)
DCN	decorin	SELP	selectin P (granule membrane protein 140kDa, antigen CD62)
EDN3	endothelin 3	SNFT	Jun dimerization protein p21SNFT
EGFR	epidermal growth factor receptor	TGFBR2	transforming growth factor, beta receptor II
FBLN1	fibulin 1	THBS1	thrombospondin 1
FBN1	fibrillin 1	TPSAB1	tryptase alpha/beta 1
KITLG	KIT ligand	VWF	von Willebrand factor

Red: increase, green: decrease, number under each shape is the fold change. *: Duplicates -Gene/ Protein/ Chemical identifiers marked with an asterisk indicate that multiple identifiers in the dataset file map to a single gene/ chemical in the Global Molecular Network.

Figure 4. Cardiovascular dysfunction and disorders identified by IPA with glossary for gene symbols in the table below.

bly, structural integrity, and function.[20] Multimerin,[21] versican,[22] lumican,[23] and vitronectin[24] are important ECM glycoproteins that are also downregulated in the MR heart. These molecules link microfibrils, such as fibrillin, elastic fibers, and collagen, to cell surfaces, as indicated by adhesion of fibronectin matrix to versican defects in the IPA map.

It is of note that integrin α_v is also downregulated. Integrins mechanically link the cytoskeleton to the ECM in cardiomyocytes and are important in transducing mechanical signals to the cardiomyocyte. Integrins, including integrin α_v, as well as phosphorylation of focal adhesion kinase (FAK), have been shown to be upregulated in pressure overload.[25] In 4-week MR dogs, we found a decrease in FAK tyrosine phosphorylation along with FAK interaction with adapter and cytoskeletal proteins p130^{Cas} and paxillin.[26] In contrast, FAK phosphorylation is upregulated in pressure overload, and its silencing attenuates the increase in collagen content and fibrosis in response to pressure overload.[27] IPA identified

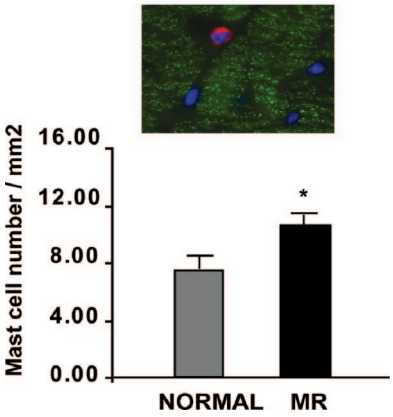

Figure 5. Representative mast cell number with chymase antibody in red in MR and mast cell numbers in MR vs normal dogs. MR: n=5; normal: n=4.

downregulation of epidermal growth factor receptor in 4-month MR LVs. Epidermal growth factor receptor stimulation triggers a cascade of events that affect cell morphology, FAK phosphorylation, and phosphorylation of many cytoskeletal proteins and has been associated with growth and aggressiveness of tumors.[28] A loss of ECM and its signals to the cell surface could result in decreased integrin and epidermal growth factor receptor expression in MR.

Central to the decrease in ECM component synthesis is the downregulation of the group complex of TGF-β and of CTGF, which are both increased in models of pressure overload.[29] TGF-β regulates decorin, fibulin, and fibrillin production,[30,31] and downregulation of the TGF-β group complex was verified by significant decreases in phosphorylated smad2 and TGF-β_1 activity in the MR LVs. CTGF mediates interactions with growth factors, integrins, and ECM components and is required for ECM production. In the CTGF knockout mouse, a decrease is seen in chondrocyte proliferation, tensile strength of cartilage, and growth plate angiogenesis.[32] CTGF also mediates TGF-β fibrotic responses by suppression of smad7 transcription,[33] and binding of CTGF to TGF-β enhances TGF-β_1 activity.[34] Finally, a 3-fold decrease is seen in PAI-1 expression, a principal inhibitor of plasminogen activators that promotes fibrosis by preventing MMP activation and ECM degradation by plasminogen activators and plasmin.[35] PAI-1 is upregulated markedly early in the course of pressure overload in the mouse heart.[36] Thus, IPA identified downregulation of multiple growth factors that are central to ECM integrity.

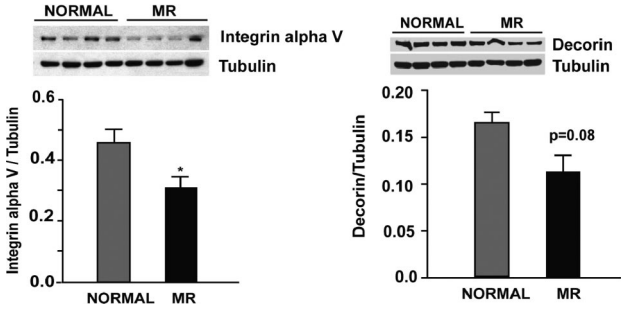

Figure 6. Western blot of integrin α_V and decorin in normal vs 4-month MR dog. *$P<0.05$. MR: n=5; normal: n=4.

IPA also identified marked upregulation of the chemokine proplatelet basic protein,[37] adhesion molecules selectin L and selectin P, and stem cell factor KITLG, resulting in links to vascular injury, myocardial infarction, degranulation of granulocytes, and mast cells (Figure 5). This inflammatory feature is consistent with our finding of an early and persistent increase in mast cells and chymase activity in the MR dog.[4] Mast cells contain a collection of cytokines and proteolytic enzymes, including tryptase and chymase, which activate MMPs.[38] Indeed, mast cell tumors in dogs have increased MMP-2 and -9 activity that predicts tumor invasion and histological score.[39] In the volume overload of aortocaval fistula in the rat, mast cell stabilization attenuates LV dilatation, presumably by inhibiting MMP activation.[40] Thus, influx of mast cells and other inflammatory cells could be responsible for the increase in MMPs as well as their activation via their inflammatory cell proteases, but the increase in MMP mRNA also suggests production from resident cardiac cells such as fibroblasts.

Increased interstitial fibrosis, replacement fibrosis, and perivascular fibrosis have been identified in many forms of heart failure, especially in response to pressure overload. In contrast, here we report downregulation of profibrotic factors in MR in the face of an inflammatory gene and mast cell response. Although this may allow for a more compliant LV to accommodate the volume load, the loss of collagen and noncollagen ECM components may permit excessive LV dilatation. The loss of collagen has been a consistent finding in all of our studies of this dog model for up to 6 months after MR induction.[4] Beeri and coworkers[41] reported greater activation of MT-1 MMP in the remote region of a sheep model of apical infarction combined with LV to left atrial shunt of 30% compared with infarct alone, suggesting that the additional stretch of LV regurgitant shunt activated MMPs. This normalized at a later time point along with upregulation of tissue inhibitors of MMPs. Thus, our time point of 4 months may be relatively early in the time course in this model, and fibrosis may ensue at a later stage of MR, perhaps at 1 year or later.

A limitation of the this study is that a parametric test for analyzing fold gene changes with the small sample of 4 MR dogs represents a problem when it is not possible to verify that the difference data have a normal distribution. Nevertheless, protein confirmation of downregulation of the TGF-β receptor and signaling system supports the contention that this low-pressure type of volume overload induces molecular signals not only for increased MMPs but also for decreased synthesis of noncollagen ECM proteins and their growth factors. Although this may initially allow for a more compliant LV chamber, over time, persistent ECM loss leads to myocyte slippage, apoptosis,[42] and cardiomyocyte dysfunction. Taken together, molecular signals that decrease synthesis in the face of increased degradation of ECM could explain why antifibrotic drugs such as angiotensin-converting enzyme inhibitors and angiotensin II receptor blockers do not attenuate LV dilatation and ECM loss in the canine model of isolated MR. These findings call for a new treatment paradigm that addresses ECM loss to attenuate progressive LV dilatation in isolated MR.

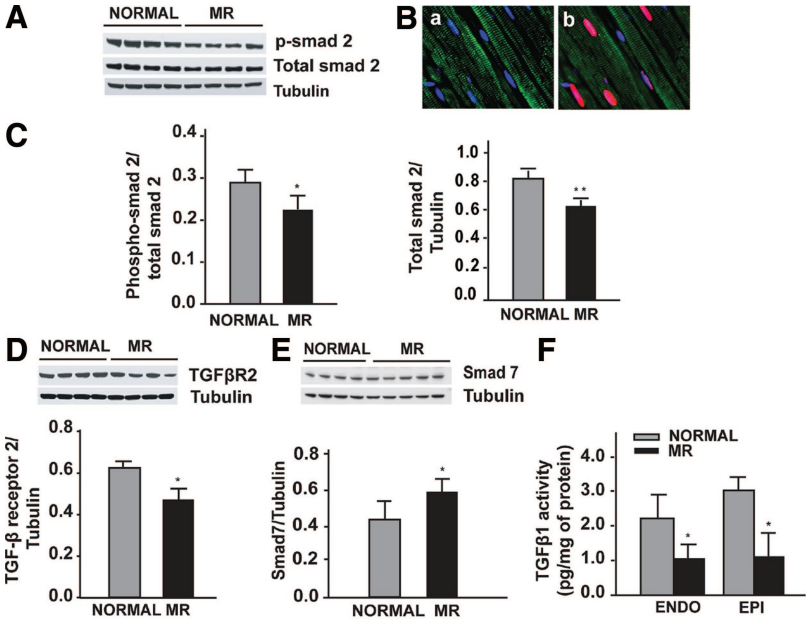

Figure 7. Western blot of phospho-smad2 (p-smad 2) in normal vs MR dogs (A) and immunohistochemistry demonstrating nuclear location of phospho-smad2 (B); a, DAPI; b, phospho-smad2 merged with DAPI. C, Quantification of phospho-smad2/total smad2 and total-smad2/tubulin. D and E, Western blot and quantification of TGF-βR2 (D) and smad7 (E) in LV endocardium in normal vs MR dogs. F, LV tissue TGF-β activity in 4-month MR dogs vs normal dogs. $^{*}P<0.05$, $^{**}P<0.01$. MR, n=5; normal, n=4.

Sources of Funding

This study is supported by the Department of Veteran Affairs (Dr L.J. Dell'Italia) and the National Heart, Lung, and Blood Institute Specialized Center of Clinically Oriented Research in Cardiac Dysfunction (P50HL077100).

Disclosures

None.

References

1. LeGrice IJ, Smaill BH, Chai LZ, Edgar SG, Gavin JB, Hunter PJ. Laminar structure of the heart: ventricular myocyte arrangement and connective tissue architecture in the dog. *Am J Physiol*. 1995;269: H571–H582.
2. Sasayama S, Ross J Jr, Franklin D, Bloor CM, Bishop S, Dilley RB. Adaptations of the left ventricle to chronic pressure overload. *Circ Res*. 1976;38:172–178.
3. Dell'Italia LJ, Meng QC, Balcells E, Straeter-Knowlen IM, Hankes GH, Dillon R, Cartee RE, Orr R, Bishop SP, Oparil S, et al. Increased ACE and chymase-like activity in cardiac tissue of dogs with chronic mitral regurgitation. *Am J Physiol*. 1995;269:H2065–H2073.
4. Stewart JA Jr, Wei CC, Brower GL, Rynders PE, Hankes GH, Dillon AR, Lucchesi PA, Janicki JS, Dell'Italia LJ. Cardiac mast cell- and chymase-mediated matrix metalloproteinase activity and left ventricular remodeling in mitral regurgitation in the dog. *J Mol Cell Cardiol*. 2003; 35:311–319.
5. Dell'italia LJ, Balcells E, Meng QC, Su X, Schultz D, Bishop SP, Machida N, Straeter-Knowlen IM, Hankes GH, Dillon R, Cartee RE, Oparil S. Volume-overload cardiac hypertrophy is unaffected by ACE inhibitor treatment in dogs. *Am J Physiol*. 1997;273:H961–H970.
6. Ryan TD, Rothstein EC, Aban I, Tallaj JA, Husain A, Lucchesi PA, Dell'Italia LJ. Left ventricular eccentric remodeling and matrix loss are mediated by bradykinin and precede cardiomyocyte elongation in rats with volume overload. *J Am Coll Cardiol*. 2007;49:811–821.
7. Borer JS, Bonow RO. Contemporary approach to aortic and mitral regurgitation. *Circulation*. 2003;108:2432–2438.
8. Nemoto S, Hamawaki M, De Freitas G, Carabello BA. Differential effects of the angiotensin-converting enzyme inhibitor lisinopril versus the beta-adrenergic receptor blocker atenolol on hemodynamics and left ventricular contractile function in experimental mitral regurgitation. *J Am Coll Cardiol*. 2002;40:149–154.
9. Perry GJ, Wei CC, Hankes GH, Dillon SR, Rynders P, Mukherjee R, Spinale FG, Dell'Italia LJ. Angiotensin II receptor blockade does not improve left ventricular function and remodeling in subacute mitral regurgitation in the dog. *J Am Coll Cardiol*. 2002;39:1374–1379.
10. Chancey AL, Brower GL, Peterson JT, Janicki JS. Effects of matrix metalloproteinase inhibition on ventricular remodeling due to volume overload. *Circulation*. 2002;105:1983–1988.
11. Spinale FG, Coker ML, Krombach SR, Mukherjee R, Hallak H, Houck WV, Clair MJ, Kribbs SB, Johnson LL, Peterson JT, Zile MR. Matrix metalloproteinase inhibition during the development of congestive heart failure: effects on left ventricular dimensions and function. *Circ Res*. 1999;85:364–376.
12. Edwards CA, O'Brien WD Jr. Modified assay for determination of hydroxyproline in a tissue hydrolyzate. *Clin Chim Acta*. 1980;104: 161–167.
13. Tallaj J, Wei CC, Hankes GH, Holland M, Rynders P, Dillon AR, Ardell JL, Armour JA, Lucchesi PA, Dell'Italia LJ. Beta1-adrenergic receptor blockade attenuates angiotensin II–mediated catecholamine release into the cardiac interstitium in mitral regurgitation. *Circulation*. 2003;108: 225–230.
14. Bianco P, Fisher LW, Young MF, Termine JD, Robey PG. Expression and localization of the two small proteoglycans biglycan and decorin in developing human skeletal and non-skeletal tissues. *J Histochem Cytochem*. 1990;38:1549–1563.
15. Thieszen SL, Rosenquist TH. Expression of collagens and decorin during aortic arch artery development: implications for matrix pattern formation. *Matrix Biol*. 1995;14:573–582.
16. Sini P, Denti A, Tira ME, Balduini C. Role of decorin on in vitro fibrillogenesis of type I collagen. *Glycoconj J*. 1997;14:871–874.
17. Weis SM, Zimmerman SD, Shah M, Covell JW, Omens JH, Ross J Jr, Dalton N, Jones Y, Reed CC, Iozzo RV, McCulloch AD. A role for decorin in the remodeling of myocardial infarction. *Matrix Biol*. 2005; 24:313–324.
18. Bouzeghrane F, Reinhardt DP, Reudelhuber TL, Thibault G. Enhanced expression of fibrillin-1, a constituent of the myocardial extracellular matrix in fibrosis. *Am J Physiol*. 2005;289:H982–H991.
19. Mellody KT, Freeman LJ, Baldock C, Jowitt TA, Siegler V, Raynal BD, Cain SA, Wess TJ, Shuttleworth CA, Kielty CM. Marfan syndrome-causing mutations in fibrillin-1 result in gross morphological alterations and highlight the structural importance of the second hybrid domain. *J Biol Chem*. 2006;281:31854–31862.
20. Argraves WS, Greene LM, Cooley MA, Gallagher WM. Fibulins: physiological and disease perspectives. *EMBO Rep*. 2003;4:1127–1131.
21. Doliana R, Canton A, Buciotti F, Mongiat M, Bonalodo P, Colombatti A. Structure, chromosomal localization, and promoter analysis of the human elastin microfibril interface located protein (EMILIN) gene. *J Biol Chem*. 2000;275:785–792.
22. Wight TN, Merrilees MJ. Proteoglycans in atherosclerosis and restenosis: key roles for versican. *Circ Res*. 2004;94:1158–1167.
23. Ying S, Shiraishi A, Kao C, Converse RL, Funderburgh JL, Swiergiel J, Roth MR, Conrad GW, Kao W. Characterization and expression of the mouse lumican gene. *J Biol Chem*. 1997;272:30306–30313.

24. Gebb C, Hayman EG, Engvall E, Ruoslahti E. Interaction of vitronectin with collagen. *J Biol Chem*. 1986;261:16698–16703.
25. Babbit CJ, Shai S-Y, Harpf AE, Pham CG, Ross RS. Modulation of integrins and integrin signaling molecules in the pressure overloaded murine ventricle. *Histochem Cell Biol*. 2002;418:431–439.
26. Sabri A, Rafio K, Kolpakov MA, Dillon R, Dell'Italia JL. Sympathetic activation causes focal adhesion signaling alteration in early compensated volume overload attributable to isolated mitral regurgitation in the dog. *Circ Res*. 2008;102:1127–1136.
27. Clemente CFMZ, Tornatore TF, Theizen TH, Deckmann AC, Pereira TV, Lopes-Cendes I, Souza JRM, Franchini KG. Targeting focal adhesion kinase with small interfering RNA prevents and reverses load-induced cardiac hypertrophy in mice. *Circ Res*. 2007;101:1339–1348.
28. Nelson JM, Fry DW. Cytoskeletal and morphological changes associated with the specific suppression of the epidermal growth factor receptor tyrosine kinase activity in A431 human epidermoid carcinoma. *Ex Cell Res*. 1997;233:383–390.
29. Zhang YM, Bo J, Taffet GE, Chang J, Shi J, Reddy AK, Michael LH, Schneider MD, Entman ML, Schwartz RJ, Wei L. Targeted deletion of ROCK1 protects the heart against pressure overload by inhibiting reactive fibrosis. *FASEB J*. 2006;20:916–925.
30. Heimer R, Bashey RI, Kyle J, Jimenez SA. TGF-beta modulates the synthesis of proteoglycans by myocardial fibroblasts in culture. *J Mol Cell Cardiol*. 1995;27:2191–2198.
31. Rosenkranz S. TGF-β_1 and angiotensin networking in cardiac remodeling. *Cardiovasc Res*. 2004;63:423–422.
32. Ivkovic S, Yoon BS, Popoff SN, Safadi FF, Libuda DE, Stephenson RC, Daluiski A, Lyons KM. Connective tissue growth factor coordinates chondrogenesis and angiogenesis during skeletal development. *Development*. 2003;130:2779–2791.
33. Wahab NA, Weston BS, Mason RM. Modulation of the TGFbeta/Smad signaling pathway in mesangial cells by CTGF/CCN2. *Exp Cell Res*. 2005;307:305–314.
34. Abreu JG, Ketpura NI, Reversade B, De Robertis EM. Connective-tissue growth factor (CTGF) modulates cell signalling by BMP and TGF-beta. *Nat Cell Biol*. 2002;4:599–604.
35. Loskutoff DJ, Quigley JP. PAI-1, fibrosis, and the elusive provisional fibrin matrix. *J Clin Invest*. 2000;106:1441–1443.
36. Bloor CM, Nimmo L, McKirnan MD, Zhang Y, White FC. Increased gene expression of plasminogen activators and inhibitors in left ventricular hypertrophy. *Mol Cell Biochem*. 1997;176:265–271.
37. Baggiolini M. Chemokines and leukocyte traffic. *Nature*. 1998;392:565–568.
38. Caughey GH. Mast cell tryptases and chymases in inflammation and host defense. *Immunol Rev*. 2007;217:141–154.
39. Leibman NF, Lana SE, Hansen RA, Powers BE, Fettman MJ, Withrow SJ, Ogilvie GK. Identification of matrix metalloproteinases in canine cutaneous mast cell tumors. *J Vet Intern Med*. 2000;14:583–586.
40. Brower GL, Chancey AL, Thanigaraj S, Matsubara BB, Janicki JS. Cause and effect relationship between myocardial mast cell number and matrix metalloproteinase activity. *Am J Physiol*. 2002;283:H518–H525.
41. Beeri R, Yosefy C, Guerrero JL, Nesta F, Abedat S, Chaput M, del Monte F, Handschumancher MD, Stroud R, Sullivan S, Pugatsch T, Gilon D, Vlahakes GJ, Spinale FG, Hajjar RJ, Levine RA. Mitral regurgitation augments post-myocardial infarction remodeling failure of hypertrophic compensation. *J Am Coll Cardiol*. 2008;29:51:487–489.
42. Michel JB. Anoikis in the cardiovascular system: known and unknown extracellular mediators. *Arterioscler Thromb Vasc Biol*. 2003;23:2146–2154.

CLINICAL PERSPECTIVE

Evidence from the dog model of isolated mitral regurgitation suggests that persistent loss of interstitial collagen is central to chronic eccentric left ventricular and cardiomyocyte remodeling, but the molecular basis remains unclear. The findings of the current investigation demonstrating a decrease in molecular signals that decrease synthesis of matrix in the face of increased matrix degradation could explain why antifibrotic drugs such as angiotensin-converting enzyme inhibitors and angiotensin II type 1 receptor blockers do not attenuate left ventricular dilatation and matrix loss in the canine model of isolated mitral regurgitation and in some limited patient studies. This animal model is especially relevant because there is currently no recommended medical therapy available to attenuate left ventricular remodeling and thereby delay the need for valve surgery in patients with isolated mitral regurgitation. These findings may call for a new treatment paradigm that addresses matrix loss to attenuate progressive left ventricular dilatation in isolated mitral regurgitation.